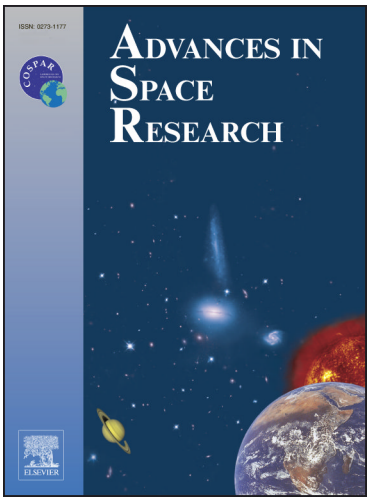

Site analysis in the Argentinean Andean region for the placement of astrophysical observatories and solar photovoltaic power plants. The case of the "Leoncito 2" site

M.M. Freire, L.S. Della Ceca, M.I. Micheletti, I. Novara, B. Garcia, A. Mancilla, GM. Salum, E. Crinó, RD. Piacentini

PII: S0273-1177(19)30283-2
DOI: https://doi.org/10.1016/j.asr.2019.04.023
Reference: JASR 14228

To appear in: *Advances in Space Research*

Received Date: 4 January 2019
Revised Date: 13 April 2019
Accepted Date: 22 April 2019

Please cite this article as: Freire, M.M., Della Ceca, L.S., Micheletti, M.I., Novara, I., Garcia, B., Mancilla, A., Salum, GM., Crinó, E., Piacentini, RD., Site analysis in the Argentinean Andean region for the placement of astrophysical observatories and solar photovoltaic power plants. The case of the "Leoncito 2" site, *Advances in Space Research* (2019), doi: https://doi.org/10.1016/j.asr.2019.04.023

Site analysis in the Argentinean Andean region for the placement of astrophysical observatories and solar photovoltaic power plants. The case of the "Leoncito 2" site

Freire M. M.[1], Della Ceca L.S.[1], Micheletti M.I. [1,2], Novara I.[1], Garcia B.[4, 5], Mancilla A.[4], Salum G.M.[6], Crinó E.[7] and Piacentini R.D.[1,5]

[1]Área Física de la Atmósfera, Radiación Solar y Astropartículas, Instituto de Física de Rosario IFIR – CONICET/Universidad Nacional de Rosario, 210 (bis) 27 de Febrero Bv, Rosario S2000EZP, Argentina.

[2] Facultad de Ciencias Bioquimicas y Farmaceúticas (FBioyF) Universidad Nacional de Rosario, 531 Suipacha St, Rosario S2000LRK, Argentina.

[3] Facultad de Ingeniería, Ingeniería y Agrimensura (FCEIA), Universidad Nacional de Rosario, 250 Pellegrini Av., Rosario S2000, Argentina.

[4] Instituto en Tecnología de Detección y Astropartículas CONICET-CNEA-UNSAM, 122 Figeroa Alcorta St., Godoy Cruz M5501CID, Mendoza, Argentina.

[5] Universidad Tecnológica Nacional, Facultad Regional Mendoza (UTN FRM), 273 Rodriguez St., Mendoza City M5502AJE, Argentina.

[6]Escuela de Ciencias Biológicas e Ingeniería, Universidad YachayTech, Hacienda San José n/n, San Miguel de Urcuquí 100650, Ecuador, Hacienda San José n/n, San Miguel deUrcuquí 100650, Ecuador.

[7]Facultad de Ciencias Físico-Matématicas, Universidad Nacional de San Luis, 950 Ejercito de los Andes St, San Luis D5700HHW, San Luis, Argentina.

Keywords:

PV powerplants, Astrophysical Observatories, Argentinean Andean atmosphere.

E-mail adresses of authors:

Freire M: freire@ifir-conicet.gov.ar

Della Ceca L.: dellaceca.lara@gmail.com

Micheletti M.I: maria.i.micheletti@gmail.com

Novara I.: ivasiton@yahoo.com.ar

Garcia B.: beatrizgarciautn@gmail.com

Mancilla A.: alexismancilla@gmail.com

Crinó E.: ecrino@gmail.com

Piacentini: ruben.piacentini@gmail.co

Corresponding autor: Freire Martín Miguel (freire@ifir-conicet.gov.ar) or Rubén D. Piacentini, (ruben.piacentini@gmail.com). Telephone number: +54 (0341) 4853200 / 4853222. Instituto de Física Rosario (CONICET – Universidad Nacional de Rosario), Bv 27 de Febrero 210 bis, S2000EZP, Rosario, Argentina.

Abstract

After a detailed search for possible sites where to place astrophysical facilities in Argentinean Andean region, a location labeled as LEO 2 (31°24'22" S, 69º29'32" W, 1630 masl)is proposed. It is placed near the largest Astronomical Observatory of Argentina: Complejo AStronómico El LEOncito (CASLEO). Its advantages are: a good altitude to detect the maximum development of cosmic ray showers, high spectral transmittance to UV and visible ranges, very low aerosol content (mean particle concentration measured at ground with an optical particle counter $PM_{2.5}$ = 1.52 µg.m^{-3}and $PM_{>2.5}$= 6.83 µg.m^{-3}, mean Aerosol Optical Depth at 550 nm = 0.027 (measured from space using the SeaWiFS instrument on board of the SeaStar NASA satellite). A local meteorological analysis was done, using data measured in situ, which shows a typical desertic site with the following *mean annual* (*std. dev.*) values:mean annual temperature 18.93 (7.66) ºC, mean annual relative humidity 28.76 (20.55)%, low/ moderate mean annual average wind speed 11.63 (8.78) Km/h, low mean water content (0.73 cm) and rather low mean cloud coverage fraction (cloud coverage fraction): 0.29 (0.02) (for the period 2003 - 2016 from Aqua/NASA satellite MODIS device) and 0.25 (0.01) (for the period 2000 – 2016, Terra/NASA satellite MODIS device).Concerning the conditions for the placement of photovoltaic solar power plants, some positive aspects that can be remarked are a large rather flat available surface (336 Km^2) with very good levels of annual mean horizontal solar irradiation: Global (2334 KWh.m^{-2}*per year*), Direct(3127 KWh.m^{-2}*per year*) and Diffuse (394 KWh.m^{-2}*per year*). Optimum angle to place solar panels at this site is determined and the global tilted solar irradiation is calculated (2689 KWh.m^{-2}*per year*). In comparison with an African (Ouarzazate, Morocco) and Asian (Dubai) sites, the analysed site present better annual irradiation levels being the Global horizontal irradiation at the Argentinean site 8.1% and 10.3% higher than those calculated for the African and Asian site respectively. Also, a comparison is made of different solar cells (monocrystalline Si, polycrystalline Si and perovskite), through the calculation of the generated photocurrent (mean produced solar photovoltaic current per unit cell surface), considering the atmospheric and solar radiation parameters found for the studied site. We thus conclude that the proposed site in the Andes range is well suited for the placement of Astrophysical facilities, as well as Photovoltaic solar power plants.

1. Introduction

Currently, experimental detection and analysis of astroparticles (also called *cosmic rays*) are being carried on in different places of the world. Large collaborations between many countries and scientific institutions make possible to build giant ground-based arrays of telescopes with increasing sensivity and accuracy. Since the atmosphere acts as a first detector of astroparticles, the sites to place those facilities need specific atmospheric and geographical conditions: to be far away from considerable pollution sources, to present very clean atmospheric conditions (low aerosol content and cloud coverage), to be located at an altitude range corresponding to the maximum development of the cosmic ray shower (maximum production of "secondary" particles originated during the "cascade" process originated by the "primary" cosmic ray when it enters the atmosphere and interacts with it). These specific conditions, added to others like site accessibility and other logistic issues, make the election of a suitable site a very challenging task.

In the past decade, the Cherenkov Telescope Array (CTA), an astrophysical observatory devoted to the detection of high energy gamma radiation (from 100GeV to 10TeV) has emerged as a mega international project involving participation of 32 countries (www.cta-observatory.org). This project includes the construction of two observatories: one in the Northern hemisphere and the other in the Southern one. After its beginnings in 2005, the search for sites around the world was carried on, looking for appropriate atmospheric and topographic conditions to house the observatories. This stage concluded with a total of 9 sites chosen to be studied to determine their detailed characteristics (5 on the Southern hemisphere and the other 4 on the Northern one). Two of these sites were located in the Argentinean Andean region: one near San Antonio de los Cobres (referred as SAC) in Salta province (24º02'43"S, 66º14'06"W, 3607m asl) and the other one near the Complejo AStronómico El LEOncito CASLEO (referred as LEO) in San Juan province (31º04'48"S,69º04'48"S, 2670m asl). Various studies have been performed to characterize the Argentinean candidates (Piacentini et al. 2016, Maier G. et al., 2015, Allekote I., 2013, Otero L. et al., 2013). While the first studies were taking place, a third candidate was considered: an alternative site in the area of LEO, but at a lower altitude. Because this third site is also located near CASLEO it was referred as LEO 2 (31°24'22"S, 69º29'32"W, 1630 m asl, see Figure 1.a.left). Although the site finally selected by the CTA consortium is placed in the Chilean Andean side, the information obtained during the selection process

showed that the Argentinean candidates are really good alternatives for future astroparticle projects.

In the Argentinean Andean region, several national and international astronomical/ astrophysical research projects are already running. The Pierre Auger Observatory (www.auger.org) in Mendoza Province, near the city of Malargüe (35°27'48"S, 69°35'05" W, 1420 m asl) is an international mega-project for the detection of extraterrestrial massive particles, fully functional since 2008. The Large Latin-American Milimeter Array (LLAMA) project (http://www.iar.unlp.edu.ar/llama-web/english.html) a joint Argentinean-Brazilean initiative, has been installed in Altos Chorrillos (66º28'29.4"W, -24º 11'31.4"S, 4.820 m asl), 28 km away from San Antonio de los Cobres. It is a large single telescope (12 m diameter) to observe the universe at millimetric and submillimetric wavelengths, designed also to operate in conjunction with the Atacama-Large Millimeter/Submillimeter Array (ALMA), placed in the Chilean Atacama desert (23º01'09"S, 67º45'11"O, 5058 m asl). The Astronomical complex CASLEO mentioned above is the largest astronomic observatory complex in Argentina. Since its opening in 1986 to the date, it has been operative continuously for more than 30 years.

(a)

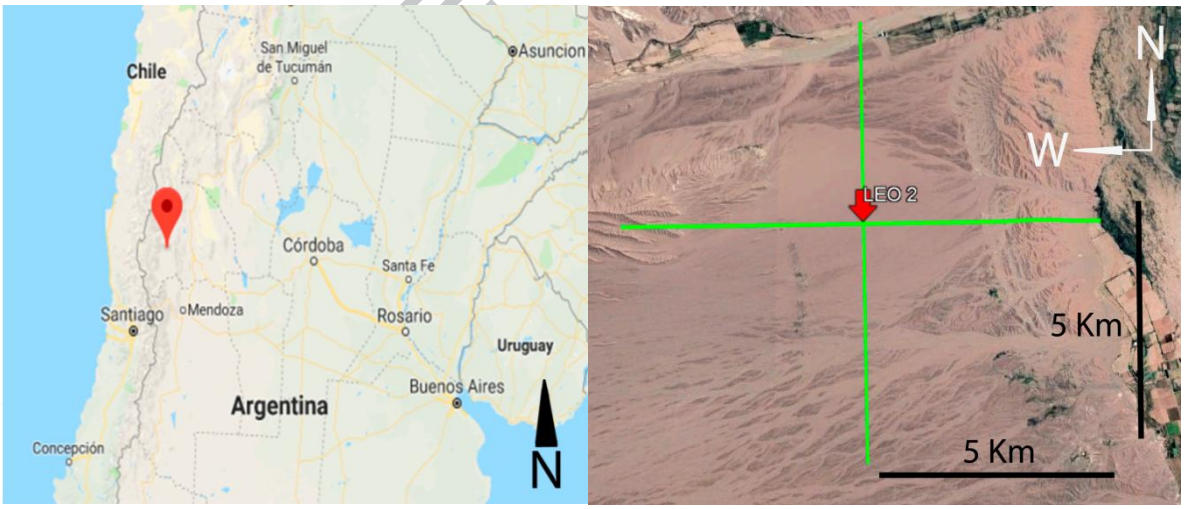

(b)

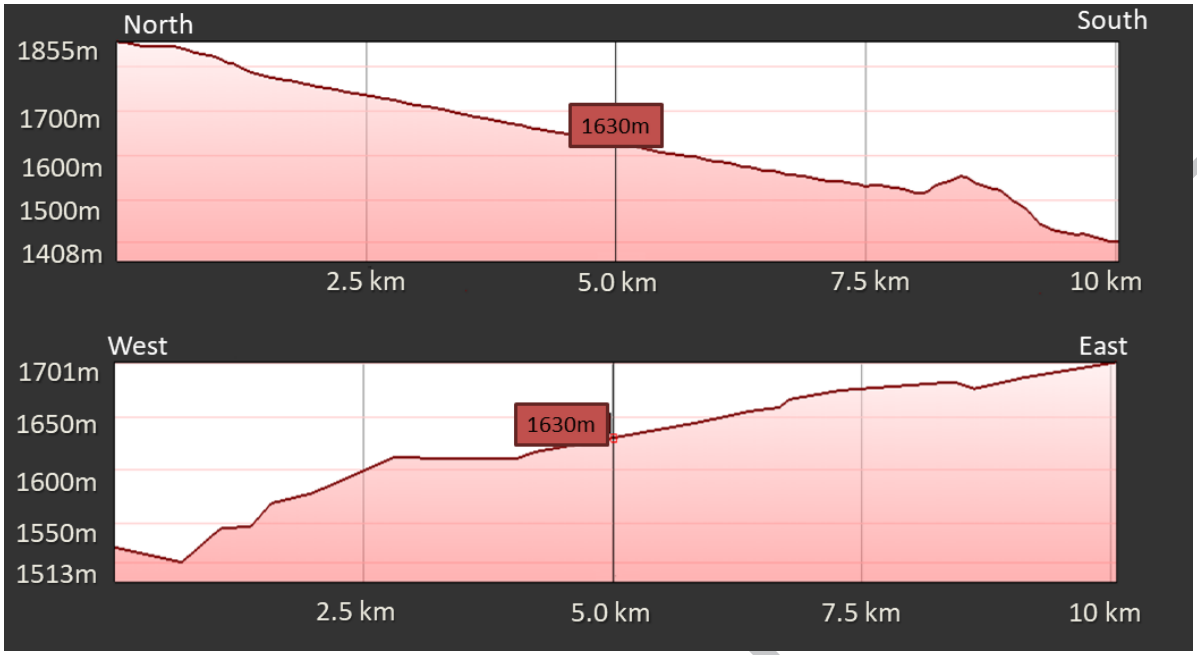

Figure 1.(a).left: The geographical position of the LEO 2 site is indicated by the red symbol. (a).right: Details of the geography of the proposed site LEO 2 site at the Argentinean Andes range (31°24'22"S, 69º29'32"W, 1630 m asl). (b.)top:10 Km elevation profile in the North (on the left) to South (on the right) direction (where LEO 2 is also placed at 5 Km from the selected origin). (b).bottom: Elevation profiles: 10 Km elevation profile in the West (left) to East (right) direction. LEO 2 site is placed at 5 Km from the selected origin. Source: Google Earth Pro.

Figure 1.(a).left presents the geographical location of the LEO 2 site in Argentina and Figure 1.(a).right, shows a satellite image over the LEO 2 region, here the straight lines extend over 10 Km and shows North-South and West-East directions. Figure 1.(b) shows that LEO 2 is a plateau with slight inclinations. In particular Figure 1.(b).top, describes the elevation profile in the North-South direction and Figure 1.(b).bottom, the West-East one. Both profiles, calculated from the corresponding straight lines shown in Figure 1.(a).right, can be approximated by linear functions, whose slopes can be considered as a measure of the site inclination. The mean slope of the site in the West-East direction is 2º03' while its value in the North-South direction is 1º08'. Figure 2 shows that the inclined flat area of the LEO 2 site previously analyzed (figure 1.(a).right and Figure 1 (b) top and bottom) can be extended over a reasonably large area of 336 Km^2.

Figure 2: Estimation of useable area of the site LEO 2 for the possible placement of Astrophysical observatories and Solar photovoltaic power plants. This plateau extends over an estimated area of 336 Km^2, with a perimeter of 85.8 Km. (Image: adapted from Google Earth Pro).

In this work, main atmospheric properties of LEO 2 are presented: spectral transmittance to UV and VIS photons for typical atmospheric components, Aerosol concentration at ground level and Satellite Aerosol Optical Depth, precipitable water content, and local meteorological variables.This study follows different analyses of atmospheric properties, already done in the past (not only for Argentinean-Andean region). These previous experience includes ozone studies (Piacentini et al., 2002), aerosols concentrations (Micheletti et al., 2017; Ipiña et al., 2012), clouds (Cede et al., 2002), and solar radiation (Piacentini et al., 2002b; Cede et al., 2002b). In particular, measurements of UV and global solar irradiances at Puna of Atacama Cerro Tres Cruces (placed in the same Argentinean Andes mountain chain) are within the largest values in the world (Piacentini et al., 2003).

2 Instruments and mathematical models

For the continuous aerosol concentration measurements, a Grimm aerosol spectrometer model 1.109 (GRIMM Aerosol Technik Ainring GmbH & Co, Germany) was used. It is a portable device designed for the determination of mass (or particle) concentration of particulate matter with diameters greater than 0.25 µm ($PM_{>0.25}$). This instrument can also be used (as described in Grimm user's manual https://www.wmo-gaw-wcc-aerosol-physics.org/files/opc-grimm-model--1.108-and-1.109.pdf) *in the mode of*

"particle mass". In this case an additional size channel is arithmetically adjointed below the smallest size channel (0.22 – 0.25µm). This small size channel is primarily useful when calculating the standarized mass fractions and leads to an improved accuracy when measuring fine aerosols. The number of particles on the air sample is equal to the detected number of pulses. The size of the particle is proportional to the intensity of the registered scattering signal (a wide-angle mirror amplifies the scattering signal, improving the precision in size determination). Finally, by means of internal modeling of the device, the mass of the particles is determined. The efficiency in the particle count of this device is 90% (Heim et al., 2008).

For the local weather data acquisition, a Reinhardt Weather station was placed in LEO 2 site. In fact this station is part of the equipment used to monitor the atmosphere conditions in all Cherenkov Telescope Array candidate sites. This set of monitoring instruments is called ATMOSCOPE (Autonomous Tool for Measuring Site Condition PrEcisely) consists in: the already mentioned Reinhardt weather station (for measuring air temperature, relative humidity, pressure at ground level, wind speedand wind direction), an All Sky Camera (ASC) for the monitoring of night sky quality and a Light of Night Sky (LoNS) to monitor night sky light intensity through a B and a V band filters(Johnson-Cousin Photometric system). More details about these devices can be found elsewhere (i.e.Vincent S. 2013).

To analyze wind masses motion, the HYSPLIT4 algorithm (Draxler and Rolph, 2003) was used. This algorithm is well-known and widely used for different purposes. In this work, itwas used to determine the origin of air masses arriving to the LEO 2 site over the period in which aerosol concentration measurements were taken. With respect to the atmospheric transmittance analysis, the SMARTS2.9.5 model was used (Gueymard, 1995).

3. Results

Various atmospheric components are analyzed in the present work. The results supplied by the first aerosol concentration ground measurement performed at the site and satellite data of vertical aerosol optical depth, are presented. Also, the precipitable water content and local meteorological variables are considered, as well as a study of the atmospheric conditions (transmittance for various components) that can be derived by

using some of the previous results. This study is important to understand the attenuation characteristics of the electromagnetic radiation (in the UV and Visible ranges) of the LEO 2 atmosphere, either for its application in projects devoted to measure weak electromagnetic signals (as in the case of astrophysical observatories), or for its application in devices that perform the photovoltaic conversion of solar energy into electricity.

3.1 Aerosol concentrations measured at ground level

Aerosol concentration measurements at ground level were taken in LEO 2, using the GRIMM aerosol spectrometer described in Section 2, from 9th October to 23rd October, 2013. Previous studies on the other Argentinean candidate sites for CTA (SAC and LEO) have been already published(Piacentini et al, 2013; Piacentini et al, 2016; Della Ceca et al, 2018).

Figure 3 top shows the mean normalized mass concentrations obtained for LEO 2. It presents a bimodal function of the concentration as a function of size, showing that the fine fraction maximum occurs in the range 0.22 and 0.3 µm, as can be observed in the inside graphics of Figure 3 (that expands the lower size range), while the coarse mode maximum is within the 4-5 µm interval. Figure 3 bottom shows the behaviour of the particle concentration of aerosols, as function of the effective diameter. In Table 1 we compare the integrated values of aerosol particle concentration as function of diameter from the following lower limits: 0.5, 1 and 5 microns, with the reference values of ISO 14644-1 Class 8, defining an extremely clean air site. In all cases, the LEO 2 site has even lower values of the integrated particle concentration. Mean values and standard deviations presented in Table 1 are obtained from data recorded every 5 minutes, considering the whole measurement period. For this reason, standard deviation must be considered as the fluctuation of aerosol particle concentration during the measurement period and not as a statistical indetermination of the mean.

Table 1: Mean Particle concentrations (std. dev.) for $PM_{>0.5}$, PM_1 and PM_5 at the LEO 2 site (Obtained with Grimm 1.109 from 9th October to 23rd October 2013), in comparison with the ISO 14644-1 Class 8, particle concentration limits for the metioned fractions.

	≥ 0.5 µm	≥1 µm	≥ 5 µm
Mean (std. dev.)	750000 (744000)	190000 (270000)	8800 (19200)
Class 8	3,52E+06	832000	29300

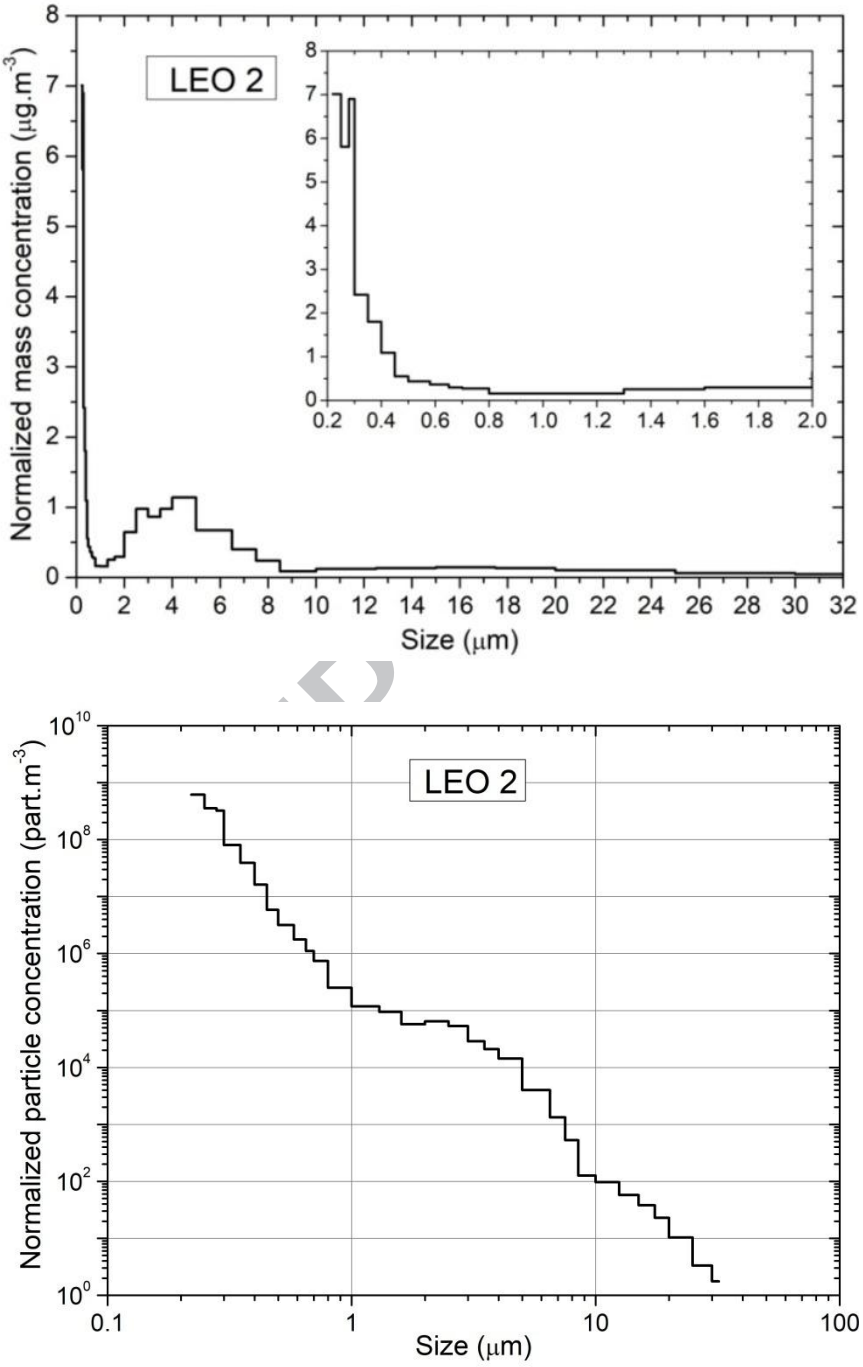

Figure 3.Top: Normalized mass concentration of aerosols as function of the aerosol size, measured from 9th October 2013 (1:02 pm, Argentina local time, UT -3 hours) to 23rd October 2013 (1:12 pm). The inner Figure expands the data measured in the range of 0.22 – 2.0 µm. Bottom:

Normalized particle concentration of aerosols as function of the aerosol size, measured in the same period. The vertical line at 5 μm is included to determine the $PM_{>5}$ fraction.

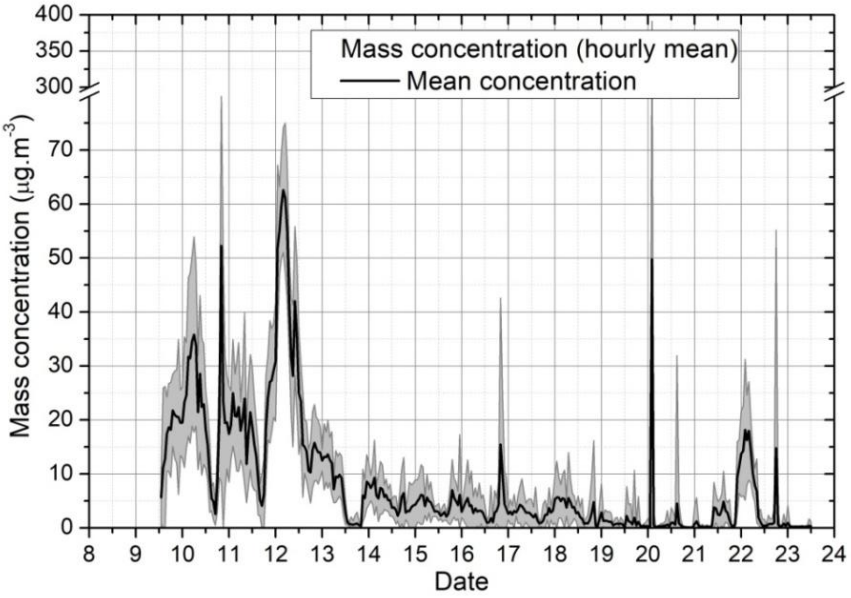

Figure 4.Hourly mean aerosol mass concentration in LEO 2 site,measured from 9th October 2013 (1:02 pm) to 23rd October 2013 (1:12 pm) (black continuous line). These mean values were calculated based in 1 minute concentration values measured by the Grimm 1.109 aersol spectrometer, within the hour XX:00 and XX:59. Grey filled area shows the region delimited by (mean ± 1 standard deviation).

Figure 4 shows a well-defined daily behavior for aerosol mass concentrations. It takes higher values during night (first hours of the day), decreasing during daylight hours. This behaviour was already observed for the other SAC and LEO studied sites, as reported in a previous work (Piacentini et al, 2016). This effect might be caused by the thermic contraction of the Planetary Boundary Layer Height (PBLH) during night hours. Assuming that the aerosol sources/ sinks are the same, both during the daytime and nighttime periods, it can be thought that the mean particle content remains constant. In this way, the reduction of the PBLH decreases the volume of the mixing layer, causing an increase in aerosol concentration.

Observing Figure 4 during the first 5 measurement days (9^{th} to 13^{th} October 2013), mass concentration takes higher values in comparison with the next 6 days (14^{th} to 19^{th}October 2013).It can be seen that during the first 5 days (*hazy period*), the mass concentration take rather high values compared to the following 6 days. Also the same happens with the absolute difference between daily maximum and minimum mass

concentration values.The following period of 6 days (*clear period*), mass concentration takes lower values and tends to decrease.

To analyze this fact and to determine possible causes for this change, several local meteorological variables are analyzed. Data was taken using the Reinhardt MWS 4M weather station, with instruments placed 3 meters above ground level. Although the local meteorology observations cover a longer period, only the period corresponding to the local aerosol concentration measurements was considered: 9th to 23rd, October 2013. The analyzed local meteorological variables are the following (absolute errors are informed between parentheses): Temperature (± 0.5 °C), relative humidity (± 2.0 %), wind speed (± 2km/h) and wind direction (± 5°).In order to analyze the effects on the aerosol mass concentrations, daily means were calculated and compared to the corresponding daily mean mass concentrations. The results are shown in Figure 5.In both cases (concentration and meteorological variables) daily mean values are obtained from 1 minute mass concentration data (measured with Grimm) and from the 5 minute data in the case of meteorological variables (measured with the Reinhardt weather station). In both cases vertical "*error bars*" shows the standard deviation for every mean, and must be understood as the dispersión of data around the daily value, and not the absolute error of the measurement. In this way, the value of the standard deviations depend on the variation of every variable within the day.

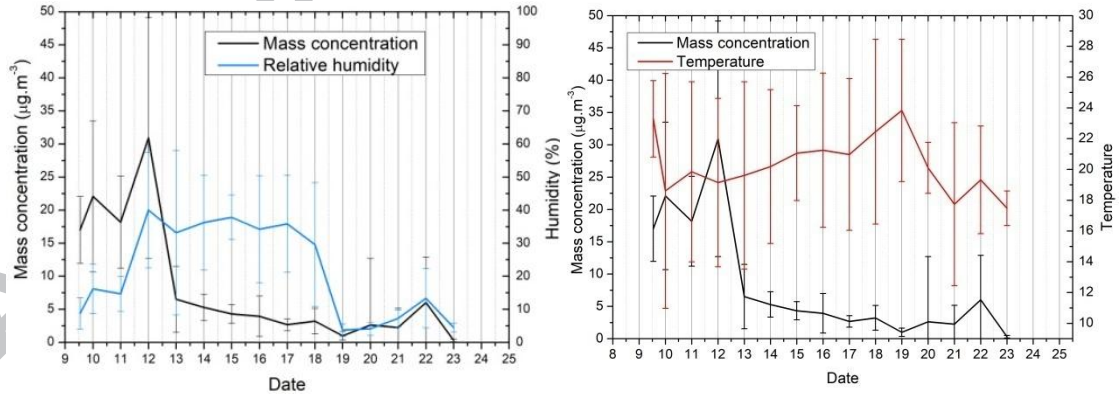

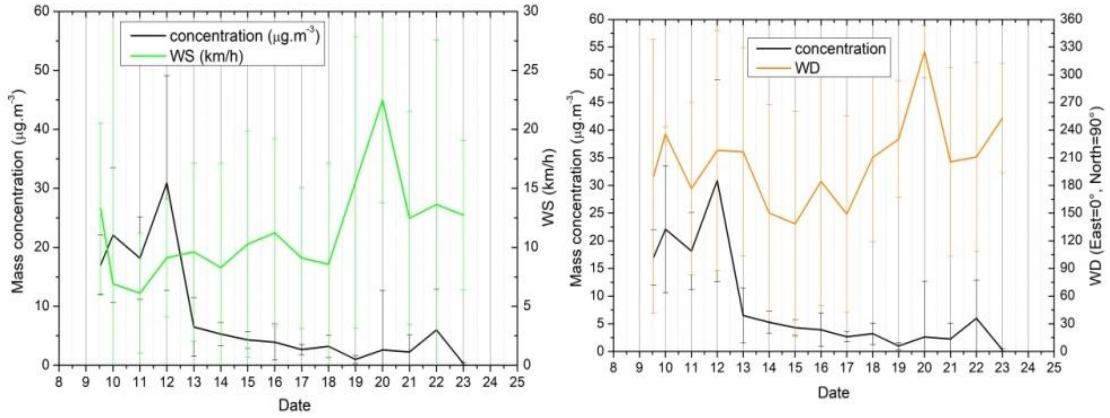

Figure 5: Correlations between local meteorological variables with aerosol mass concentrations, for the period 9th to 23rdOctober 2013: Top left: Concentration vs Relative humidity. Top right: Concentration vs Temperature. Bottom left: Concentrations wind speed (WS). Bottom right: Concentration vs wind direction (WD).

Figure 5 shows a correlation between the wind direction (Figure 5 Bottom right) and both the other meteorological variables and local aerosol concentrations, that indicates that local winds play a considerable role in driving the general atmospheric conditions at the site, including the clean/ dirty aerosol situation. In Figure 5 Bottom right, 3 periods of different wind direction ranges can be identified: 1) 9 – 13 October 2013; 2) 14 – 17 October 2013; 3) 18 – 23 October 2013. The period 1 corresponds to wind entering at the site from the West or South West direction (note that 180° is the West direction in Figure 5 Bottom right). It also corresponds to the highest aerosol concentration values measured during the in-situ data taking campaign, with low relative humidity (meaning that those wind do not carry humid air masses to the site) and with relatively high temperatures. The conjunction of the mentioned conditions allow us to infer that the wind blowing during the period 1 was the Zonda, a characteristic wind of some Argentinean Andean zones, this is a warm and dry wind that descends by brushing the mountain range. Concerning the period 2, it corresponds to winds blowing from the West or North West, as can be seen in Figure 5 Bottom right. The relative humidity maintains considerable high values during this period (Figure 5 Top left), while the aerosol mass concentration instead fall to low values. All of these conditions indicate that the aerosol and atmospheric situation in period 2 are driven by West and North West winds of Pacific Ocean origin, carrying humid air masses to the zone with low aerosol content, as also proved in previous analysis (Micheletti et al. 2017). According to Figure 5 Bottom right, in period 3 the winds turn to be southerly, initially blowing from the South-West direction, then arriving from the South-East on day

October 20th, when a peak of wind speed has been registered (Figure 5 Bottom left), and then turning again to blow from South-East directions. The humidity suddenly falls for the period 3 and the temperatures reach a maximum just before the peak in wind speed and wind direction of day October 20th. The aerosol concentrations remain low but present a small peak after the peak of the wind, suggesting that an increase in the speed of the southerly continental winds (from South-East) could lift and carry some dust during its passage. The behaviour of these variables is in accordance with the situation driven by the southerly winds.

The analysis presented indicate that the aerosol situation in the studied site is linked with the air masses arrival direction. In order to add information between air masses arriving the site during the measurement period, a HYSPLIT (Draxler and Rolph, 2004) analysis was made considering backward trajectories arriving the site (31.5°S,69.48°W) every one hour from 9th October 2013, 00 hour UTC and 23rd October 2013, 23hour UTC. The 3 periods mentioned above where considered for the HYSPLIT analysis. The corresponding results are shown in Figure 6. These results show the spatial distribution of trajectories arriving at LEO 2 at 100 m height. Considering the rural characteristic of the region and the fact that during the concentration measurement period there has been no reports of special contamination events, the most probable mechanism to explain the aerosol concentration changes is the suspension of dust particles by the action of air movement. A previous result (Micheletti et al, 2017) showed, for another East-Andean site (the Pierre Auger Observatory emplacement site) with similar characteristics than LEO 2,that air masses which have travelled above the ocean, can be associated with situations of low aerosol mass concentrations at ground level. In the mentioned work, it has been used the same Grimm 1.109 instrument during 2011 southern Winter period, under similar conditions.

The air mass analysis performed by using HYSPLIT, for the 3 periods of different wind direction situation, presented in Figure 6, is in agreement with the conclusions inferred above by considering the local meteorological variables and aerosol concentration measurements. In fact, period 1 (Figure 6 Top) shows that air masses spent more time brushing the Andean range (more proportion of orange colour contouring the mountains) before arriving from the West to the studied site, what is in accordance with the low humidity levels and the high aerosol concentrations locally measured, as well as with the characteristic behaviour of the Zonda winds. The period 2 has less influence of the

Andean dust as trajectories spend less time crossing these mountains (less red colour over them). Finally, Figure 6 Bottom shows a displacement of trajectories arrival directions to the South, in accordance with the decrease in temperature and low aerosol concentrations.

The HYSPLIT backward trajectories analysis has been extended throughout the year 2013, to deeply understand the behavior of air masses arriving at LEO 2 (see Figure 7). Each map in Figure 7 shows the frequency distribution of back-trajectories for each month of the year. They have been calculated in the same conditions as those mentioned for the results of Figure 6: 48 hours long backward trajectories arriving at the LEO 2 site every 1 hour from the 1st day of the month 00:00 local time (UT -3 h), until the last day of the same month 23:00 local time (UT -3 h). A defined behavior is observed in the air masses movement and origin:the warmer months have different behaviorsthan the coldest months of the year. During the months of January to March, and then November and December, the air masses that arrive at the LEO 2 site come from different regions, both from the ocean, and also from the continental platform (from the North-East and South-East directions). On the other hand, during the months of Winter and the first half of the spring (approximately from May to middle of October) the trajectories of the air masses travel mainly bordering the continental West coast in a North-South direction and then arriving to LEO 2 from the West. This is the typical behaviour of the Zonda wind with incidence in this region during this period. During Winter there are practically no trajectories coming from the continental shelf. while, the months of April in Autumn, and also August, September and October,in the late Winter and beginning of spring, represent a transition between the mentioned situations.

This extended analysis allows a better understanding of the aerosol concentration values obtained with the Grimm device (Figure 4): the second considered period (14^{th} – 17^{th}october 2013) presents low concentrations of aerosols in comparison with the other periods, and the HYSPLIT trajectory frequency distribution is compatible with themeasured concentrations in the Winter months. On the contrary, the first and last studied period (9^{th} – 13^{th} and 18^{th} – 23^{rd}october 2013, respectively) show more heterogeneous air masses frequency distributions.

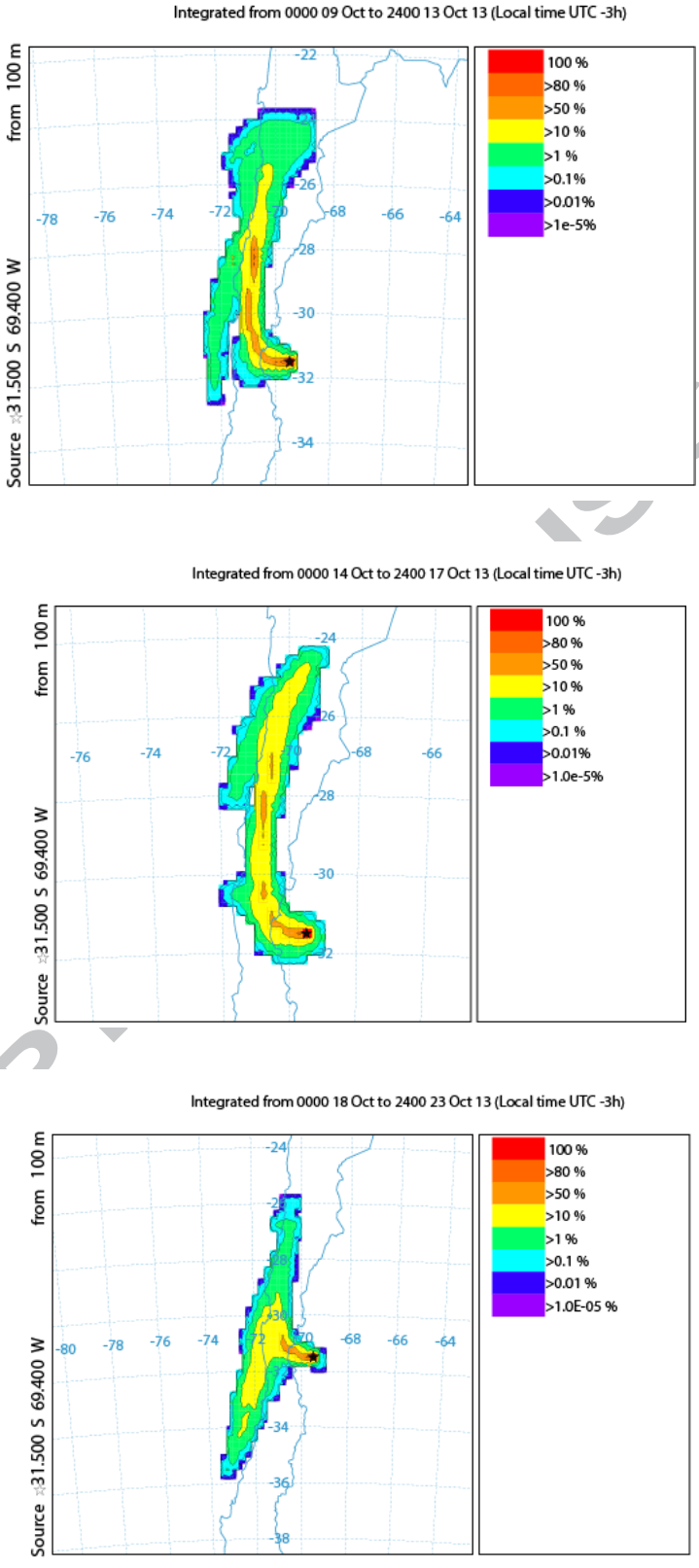

Figure 6: spatial distribution of air masses backward trajectories arriving to the LEO 2 site (31.5° S, 69.4° W, marked with a black star) at 100m agl. Each graph is made by dividing the map into a grid of 0.25°x0.25° cells, counting then the number of backward trajectories on each cell. Colors on each cell is associated with the fraction over the total number of trajectories (expressed as a

percentage). Top:Backward Trajectories for the high concentration period (9th – 13th October 2013). Middle: Backward Trajectories distribution for14th – 17thOctober 2013. Botom: Backward Trajectories distribution for 18th – 23rd October 2013.

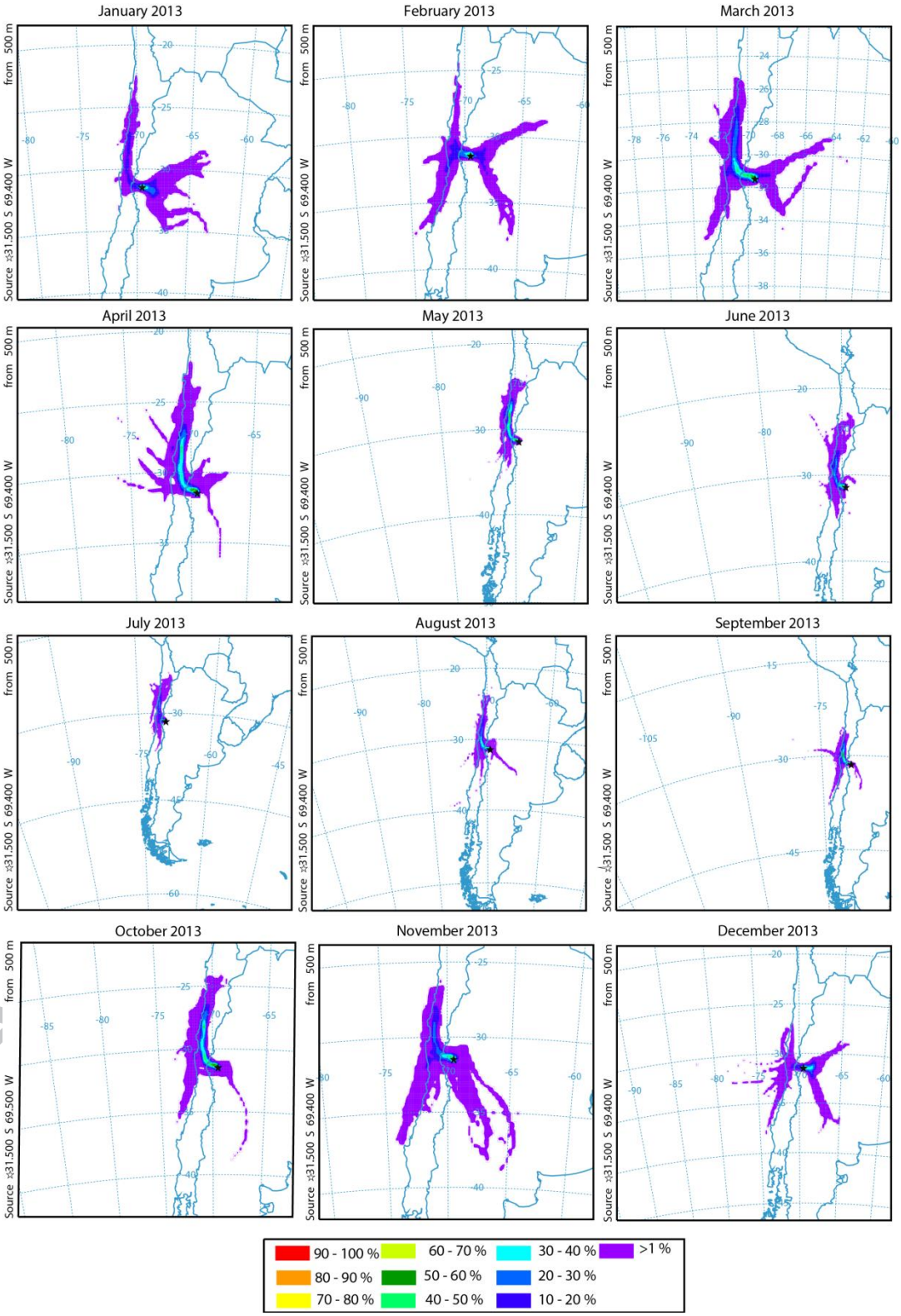

Figure 7: Monthly backward trajectories frequency plot. This analysis was made calculating 48 hours backward trajectories arriving at LEO 2 (31.5° S, 69.4° W, marked with a black star) at 500 m agl, for the year 2013, one per hour, from January to December 2013 (left to right, top to bottom). Each graph is made by dividing the map into a grid of 0.25°x0.25° cells, counting then the number of backward trajectories on each grid cell. Color scale indicates the percentage of backward trajectories on each cell (over the total number of trayectories).

3.2 Aerosol optical depth measured from space

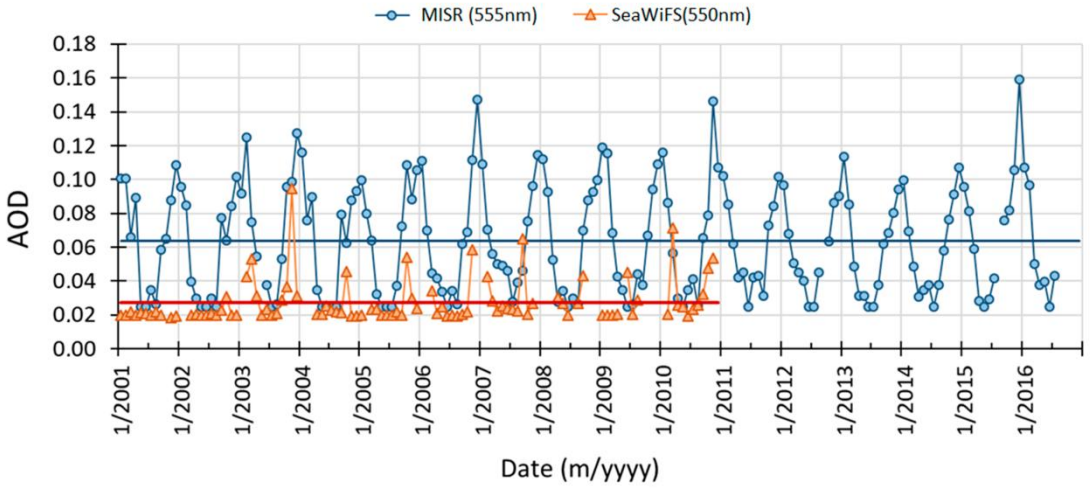

Figure 8. Aerosol Optical Depth (AOD) measured at a given wavelength, obtained with the SeaWiFS and MISR instruments on board of the SeaStar and Terra NASA satellites, respectively, in the 2001-2016 period. Data source: www.giovanni.gsfc.nasa.gov/giovanni.

Another variable that characterize the atmospheric particulate matter is the Aerosol Optical Depth ($AOD_{\lambda,X}$) , for a given wavelength (λ) and measured with a satellite sensor (X). Figure 8 shows $AOD_{\lambda,X}$ obtained with two devices: the SeaWiFS instrument (https://oceancolor.gsfc.nasa.gov/SeaWiFS) on board of the SeaStar NASA satellite (passing through LEO 2 around 12:30 p.m.), in the 2001-2010 period and MISR sensor on board of Terra/NASA satellite, in the 2001-2016 period(https://misr.jpl.nasa.gov/getData/accessData/). They show the typical oscillations along the months of the year. The minimum values are measured around the end of Southern autumn and beginning of Southern Winter and the maximum around the end of Spring and beginning of Summer. As was analyzed by Della Ceca et al. (2017),SeaWiFS data are more similar (within 10 %) than those of MISR, when compared with ground AERONET data(https://aeronet.gsfc.nasa.gov/).Mean values (± 1 standard deviation of the whole time period data) are: $AOD_{550,SW}$= 0.03 ± 0.01 for SeaWiFS and $AOD_{555,MISR}$ = 0.06

± 0.03, for MISR, having both the same spatial resolution of 0.5°x0.5°.In this way, only SeaWiFS AOD_{550nm} values are considered for further analysis. To compare AOD values obtained in LEO 2 site with other locations, we consider SeaWiFS ADO_{550nm} values for three Observatories sites: The Paranal Observatory in Chile, placed in Cerro Paranal, Atacama desert, on the west side of the same Andes mountain chain (24°37'38"S; 70°24'15"W, 2635 m asl), the Kitt Peak National Observatory, USA (31°57'30"S; 111°35'48"W, 2096 m asl), and the Paris-Meudon Solar Observatory, France (48°50'11"N; 2°20'11"E, 80 m asl). Only December and June mean monthly values for the period 2001-2011 are considered for this comparison (when Summer and Winter solstices take place). Aerosol optical depth obtained for LEO 2 during Summer has the value: $AOD_{SW,550nm}$(Dec,LEO 2) = 0.027± 0.008. It results rather low compared with those obtained for: Kitt Peak $AOD_{SW,550nm}$(Jun,Kitt Peak) = 0.04 ± 0.05, Paranal $AOD_{SW,550nm}$(Dec,Paranal) = 0.04 ± 0.02 and Paris-Meudon $AOD_{SW,550nm}$(Jun,Paris-Meudon) = 0.16 ± 0.08. For Winter, LEO 2 corresponding values are: $AOD_{SW,550nm}$(Jun,LEO 2) = 0.02 ± 0.05. And for the same period and other sites are: Kitt Peak $AOD_{SW,550nm}$(Dec,Kitt Peak) = 0.03 ± 0.01, Paranal $AOD_{SW,550nm}$(Jun,Paranal) = 0.04 ± 0.02 and Paris-Meudon $AOD_{SW,550nm}$(Dec,Paris-Meudon) = 0.13 ± 0.05.[1]

3.3 Cloud coverage

The measurements of *night* cloud fraction for LEO 2 site were already published before (Piacentini et al, 2016). This analysis was made using the All-Sky-Camera (ASC) device described before. The ASC system consist in an astronomical CCD camera with a fish eye and the necessary electronics for data acquisition (Mandat et al, 2015). This device is meant to observed and determine cloud coverage during night period, taking images every 10 minutes. The cloud fraction (CF) is determined by detecting star positions visible by the camera in every image, and comparing the ASC images with the Yale Bright Star Catalogue BSC5. The ratio (undetected stars)/(catalogue stars) gives the CF ratio. For the LEO 2 site the cloud coverage presents a sky clearness of ~70% (CF~30%) during night period (CF were measured between 8th October 2013 and 14th November 2014).

Cloud fraction all over the world is measured by MODIS/NASA instrument on board of Aqua and Terra satellites, the former passing over the Equator (and consequently other

[1]Due to the lack of data of SeaWiFS AOD for December, at Paris Solar Observatory (Meudon) the reported value was obtained interpolating data for January and November.

latitudes since its orbital period is 99 minutes in the morning and Aqua in the afternoon. We employed the MODIS Cloud Fraction monthly 1°x1° resolution mean product MOD08_M3v6.1 from Terra and MYD08_M3v6.1 from Aqua (available at http://giovanni.gsfc.nasa.gov/giovanni/).

The results are presented in Figure 9 and show cloud fraction for 17 years (from 2000 to 2016) in the case of Aqua satellite, and for 15 years (from 2002 to 2016) in the case of Terra satellite. For almost the whole period analyzed, cloud fraction values are below 0.5. Lowest cloud coverage fraction tend to appear both on Summer time and Winter time.

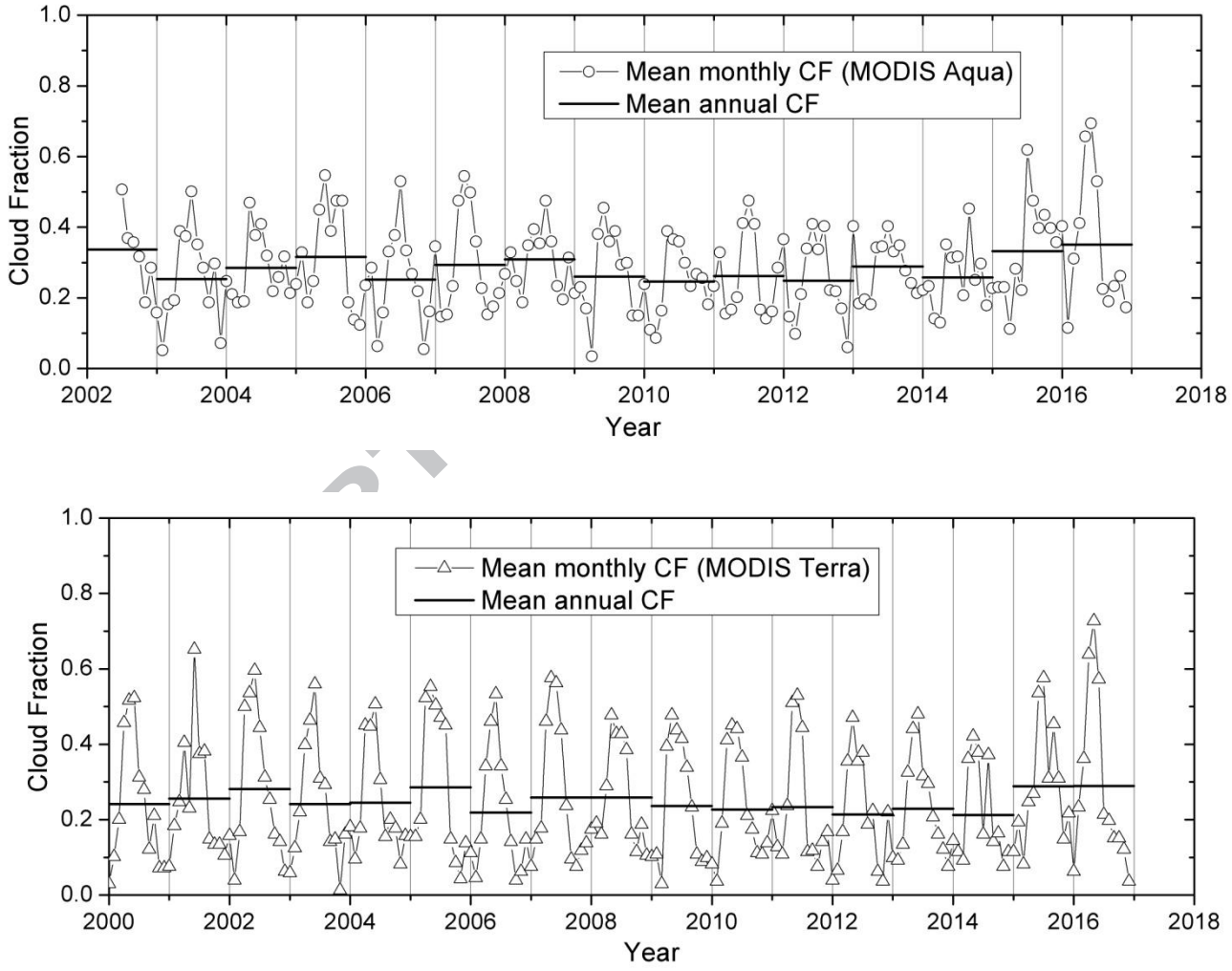

Figure 9: Cloud Fraction from Terra NASA satellite (Top) and Aqua NASA Satellite (bottom).

3.4 Precipitable water content

Precipitable water (PW) is another quantity to be studied, mainly for its influence in the radiative transmittance of the atmosphere (see Section 3.6), but also it can be an important factor to be considered, with respect to the materials employed for the construction of the astrophysical equipments (mainly iron byproducts that can be oxidized). Table 2 displays the monthly mean of PW at LEO 2 site, derived from 22 years of NASA satellite data (see: https://power.larc.nasa.gov/data-access-viewer/). PW varies from a monthly minimum in Winter of 0.38 cm to a maximum in Summer of 1.44 cm, with an annual mean of 0.80 cm.

Table 2.Monthly mean precipitable water (PW) content of the atmosphere at the LEO 2 site. Other sites are also included for comparison. The uncertainty of the measurements is estimated by SSE/NASA in 20% (Mary Jane Saddington, SSAI, NASA Langley ASDC User Services, private communication). Source: Surface Meteorology and Solar Energy/NASA.

SITE	Jan	Feb	Mar	Apr	May	Jun	Jul	Aug	Sep	Oct	Nov	Dec
LEO 2	1.44	1.36	1.17	0.75	0.55	0.45	0.38	0.41	0.50	0.63	0.85	1.17
Dubai	1.78	1.78	1.87	1.99	1.91	2.25	3.32	3.40	2.62	2.16	2.12	1.95
KittPeak	0.85	0.86	0.84	0.89	1.12	1.56	3.19	3.40	2.39	1.38	0.97	0.83
Ouarzazate	0.69	0.77	0.85	0.91	1.09	1.30	1.53	1.69	1.56	1.34	0.99	0.83
Paranal	1.37	1.41	1.27	0.93	0.77	0.67	0.58	0.58	0.61	0.69	0.81	1.06
Paris	1.14	1.10	1.24	1.39	1.83	2.25	2.50	2.50	2.14	1.91	1.46	1.25

It will be shown later (Section 3.6) that Precipitable Water content reduces the transmittance of light at large wavelength (around 700 nm). This means that the effect of water vapor on the attenuation of the typical light wavelengths detected at the Astroparticle Observatories (UV fluorescence light and UV-VIS Cherenkov radiation) is not significant. On the other hand, it indeed has to be taken into account in the photovoltaic conversion analysis, since some solar cell types can absorb photons in the NIR region. For this reason, we make a special comparison of PW content between LEO 2 and other two sites where important solar power plants are placed: Noor Solar station, 10 Km Northeast of Ouarzazatein Morocco (30°56'43"S; 6°53'54"W 1120 m asl) and the Mohammed bin Rashid Al Maktoum Solar Park, 50 Km south of city of Dubai in United Arab Emirates (25°15'52"S; 55°18'42"W, 10 m asl). As before, PW mean monthly values for December and June are compared:

The situation in Summer is the following: PW(Dec,LEO 2) = 1.17 ± 0.23 (all values expressed in cm) must be compared to PW(Jun, Dubai) = 2.25 ± 0.45 and PW(Jun, Ouarzazate) = 1.30 ± 0.3.On the other side, during Winter: PW(Jun,LEO 2) = 0.45 ± 0.11,

while PW(Dec, Dubai)= 1.95 ±0.40 and PW(Dec, Ouarzazate)= 0.8 ±0.2. So, during both periods, Summer and Winter, PW values on LEO 2 are clearly lower from those obtained for Dubai and Ouarzazate.

Also, PW content monthly values for the sites presented in Section 3.2 are included. In Summer the PW(Dec, LEO 2) = 1.17 ± 0.23 in LEO 2 is lower than those obtained for Paris-Meudon (2.25 ± 0.45) and Kitt Peak site (1.56 ± 0.31). Although, for Paranal Observatory PW content during Summer is a little lower (1.06 ± 0.20) than that obtained at the LEO 2 site, the difference is within 10%. For Winter, the PW content in LEO 2 (0.45 ± 0.08 cm) is clearly lower than the corresponding values obtained for Paris-Meudon (0.67 ± 0.13), Kitt Peak (1.25 ± 0.25) and Paranal (0.83 ± 0.17).

The annual mean value of precipitable water for LEO 2 site is quite low 0.82 cm, that can be compared with the other sites: Dubai, 2.26 cm; Kit Peak, 1.52 cm; Ouarzazate 1.13 cm; Paranal 0.89 cm; Paris-Meudon 1.73 cm.

3.5 Ground measurements of meteorological variables

The results on this section are from the analysis made with an ATMOSCOPE equipement placed at LEO 2 site. In Figure 10, mean monthly values for the main meteorological variables are presented (Temperature, relative humidity, wind speed and direction). In the same way as stated in Section 3.1, mean monthly values are obtained for the 5 minute resolution data given by the Reinhardt weather station, and the vertical "*error bars*" delimit the interval [*mean – 1 std. dev*.; *mean + 1 std. dev.*].Annual variation of temperature shows typical values corresponding to desertic site in mid latitudes. There is a clear seasonal variation between Summer and Winter, the minimum monthly mean value occurs for June(T_{min}=11.15°C), and maximum monthly mean value appears in January (T_{max}=26.51°C).

Relative humidity shows a clear seasonal behavior,the Winter months presents mean values near 20%, while the Summer months mean monthly relative humidity reaches 40%. Maximum relative humidity values registered are at most 60%.

Finally, Figure 10 (bottom left) shows monthly average local wind speed. These mean values showlow to moderate wind speeds, which can be a good factor, since higher wind speed sallows resuspension of larger particles. The coldest months (from May to August) tend to show slightly lower wind speed values in comparison with warmer

months.There is also a seasonal asymmetry, wind speed values during spring months are larger than those over autumn months, although mean monthly temperatures may be comparable for this two seasons.

Figure 10 (bottom right) shows practically no seasonal wind direction change. Mean monthly directions are in the range 170° - 215°, which corresponds to the West direction (West=180°). A more detailed observation of this Figure shows that for the coldest months (June, July and August), the standard deviation tends to have lower values (so, less variation) with respect to other months. In conclusion, the average monthly direction of local winds is practically constant throughout the year. However, with a lesser probability, other directions may occur (North, South), but at no time of the year the winds arrive from the East direction (East=0°).

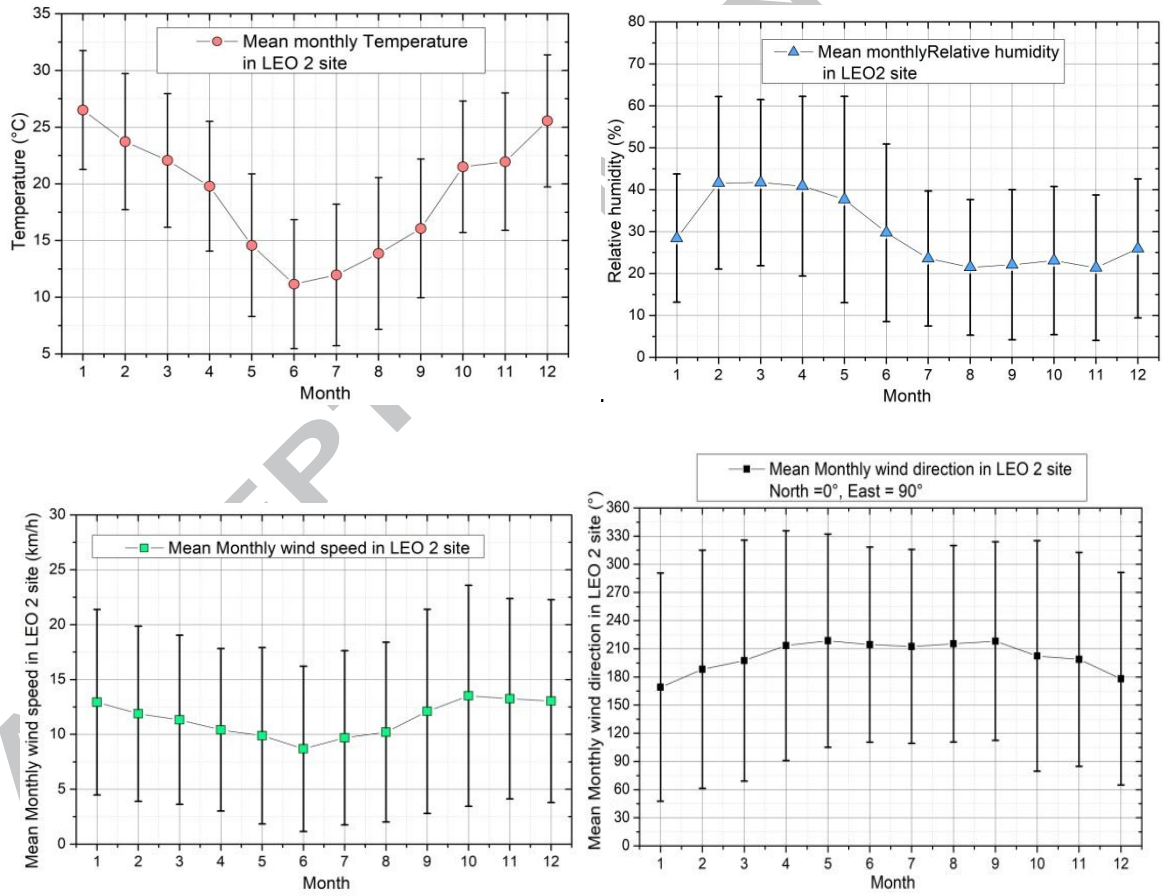

Figure 10: Mean monthly meteorological variables, measured in LEO 2 site with the Reindhard M4 weather station during 2013 – 2015. Top left: Mean monthly temperature. Top right:Mean monthly relative humidity. Bottom left:Mean monthly wind speed (WD). Bottom right: Mean monthly wind direction (WD). North = 0°, East = 90°.

3.6 Analysis of Solar radiation at LEO 2

From satellite and ground data presented before (setions 3.1, 3.2 and 3.4), it is possible to study the light attenuation caused by various atmospheric components: ozone, carbon dioxide, certain gases supposed to be uniformly mixed (CH_4, CO_2, CO, N_2, N_2O,O_2), aerosols and water vapor. The SMARTS model (V2.9.5) was used to determine surface solar spectra and the spectral transmittances of the mentioned atmospheric components (see Figure 11), Two situations are considered: Southern Summer solstice (maximum irradiance value) and southern Winter solstice (minimum irradiance value), for the local solar noon (1:00 pm local time, UT – 3hours) considering clear sky. This is the main reason why LEO 2 atmospheric parameters from data satellite were compared with other relevant sites during December and June.For this analysis the SMARTS2.9.5 modelwas executed using the following parameters (Table 3):

Table 3. Coordinates, atmospheric parameters and solar constant employed in the SMARTS algorithm (Gueymard, 1995), to obtain the UV and visible atmospheric spectral transmittances presented in Figure 11.

Latitude	(°)	-31,5	
Longitude	(°)	-69,4	
Altitude	(m asl)	1630	
		Summer	**Winter**
PrecipitableWater	(cm)	1.13	0.53
Total Ozone column	(DU)	266.7	269.1
CO_2	(ppm)	382.3	383.5
Total Solar Irradiance	(W/m^2)	1361.23	1360.34
Atmospherekind		'DESERT_MINIMUM'	
AOD (550nm)		0.027	0.022
Albedo		0.06	0.06

AOD values were obtained as a monthly mean value from SeaWiFS satellite data presented in Section 3.2 for December and June over the period 2001 – 2016. Precipitable Water values were taken from Table 2, for December and June. Total Solar Irradiance (TSI) values in Table 3 were obtained from the Total Irradiance Monitor (TIM) instrument on board of SORCE/NASA satellite

http://lasp.colorado.edu/data/sorce/tsi_data/six_hourly/sorce_tsi_L3_c06h_latest.txt). The uncertainty considered forthe values presented is 0.6W/m^2. The presented values correspond to Summer and Winter solstices 2015 (21st December and 21st June respectively).

Total Ozone column (in Dobson Units, DU) and Carbon dioxide CO_2 concentration (ppm) were obtained as a monthly mean using the database from OMI and LMS instruments on board of Aqua/NASA satellite (in particular from the Giovanni/ NASA AIRXSTM v006 data web page http://giovanni.gsfc.nasa.gov/giovanni/). These monthly means were determined considering data available in the time period 2004 – 2015. Ozone has the major attenuation effect in the UV range, mean values obtained for LEO 2 (see table 3) are rather low or at least comparable (266.7 DU in Summer and 269.1 DU in Winter) with those found for Ouarzazate site (319 DU in Summer and 298 DU in Winter) and Dubai (304 DU in Summer and 265 DU in Winter). In the case of the CO_2 total column values obtained for Ouarzazate (390 ppm in Summer and 389 ppm in Winter) and Dubai (390 ppm in Summer and 388 in Winter) are very close but rather high to those obtained for LEO 2 (382.3 ppm in Summer and 383.5 ppm in Winter).

The various atmospheric components considered, have different contributions to attenuation over the UV – VIS wavelength range. For the shorter wavelength values (λ<300nm), Ozone absorbs almost the total number of photons. For larger wavelength values, the dominant contribution to attenuation is due to the Rayleigh scattering (for almost every wavelength), followed by aerosols and O_2.Water vapor (H_2O) contribution is very important only for specific wavelength bands in the visible (VIS) and near infrared (NIR) ranges (see Figure 11). The *total* spectral transmittance is also calculated (obtained multiplying the transmittances determined for all the mentioned components).

Integrating the presented spectral transmittances over thewavelength range (280 nm – 780 nm) which contains part of the UV and the VIS range of solar radiation, the integrated transmittances, for Summer and Winter are, respectively: 67.10% and 76.08%.

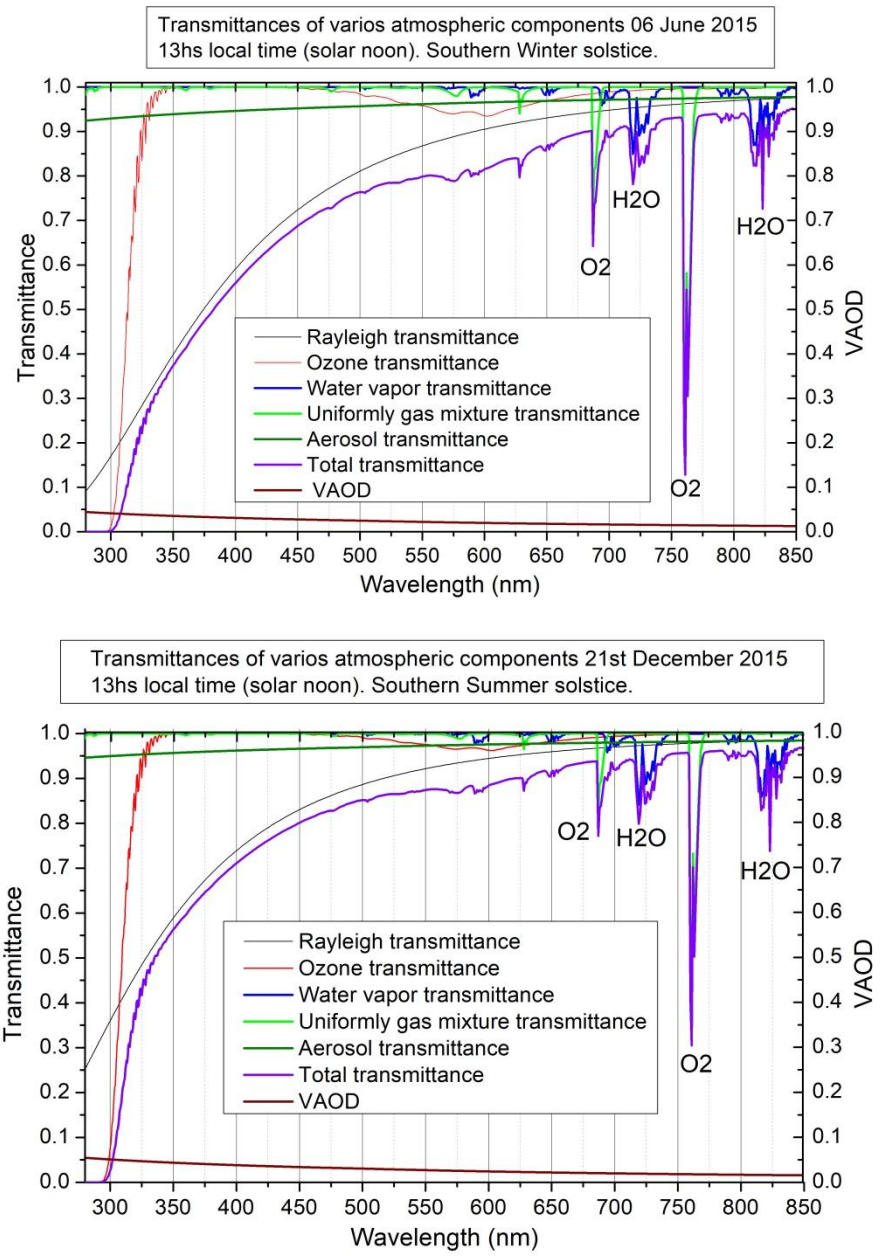

Figure 11: Transmittances for various atmospheric components calculated with SMARTS2.9.5 model in the wavelength range 280 nm – 850 nm corresponding to: Winter solstice 2015 (top) and Summer solstice 2015 (bottom). Rayleigh scattering effect is also presented. Vertical AOD (VAOD) values are displayed (calculated from data in Figure 11). Important absortion bands from O_2 and H_2O are marked. The "Uniform gas mixture" contains CH_4, CO_2, CO, N_2, N_2O, O_2 (Myers D, 2004).

3.7 Efficiency of various photovoltaic cells in LEO 2

In what follows we analyze the efficiency of energy conversion (solar to electric) taking into account the atmospheric characteristics of LEO 2. For this analysis, 3 types of solar cells are considered: *mocrystalline Si*, *policrystalline Si* and a $Ch_3NH_3PbI_3$*perovskite*

*solar cells.*For this analysis, we start from the spectral quantum efficienciesϵ_λ(SPE) of each cell type and calculate the intensity of the generated photovoltaic current surface density (or *photocurrent*) at a site with the characteristics of LEO 2, both at the Summer and Winter solstices (for the Southern hemisphere). The spectral quantum efficiency is defined as the probability that a photon of a given wavelength incident on the solar cell, generates an electric carrier (electron – hole pair), expressed as a percentage. For the monocrystalline Si and policrystalline Si, SPE were obtained from Salum M. et al. (2015) and the perovskite cell from Zhou et al. (2014).Using the SMARTS algorithm, it is possible to model the global spectral irradiance at surface, for bothsoltices, as given in Figure 12, for 21st December 2015 at 13:00hs, local time (= UT – 3h) and for 21st June 2015, 13:00hs local time. From the knowledge of the spectral quantum efficiency ϵ_λ and the spectral solar irradiance $I(\lambda)$ calculated for both solstices (Summer and Winter, local noon), the generated photovoltaic current per unit area $I_{PV,A}$ (in units of mA/cm^2) can be expressed as follows:

$$I_{PV,A} = \frac{q_e}{h.c}\int_{\lambda_1}^{\lambda_2} I(\lambda).\epsilon_\lambda.\lambda.d\lambda \quad (1)$$

being q_e the electric charge of the electron, c the speed of light in the vaccuum, h the Planck's constant, and λ the photon wavelength. In table 4 the resulting photocurrents for each type of solar cell considered are shown.

Table 4: Photocurrent intensities (mA/cm^2) for the 3 types of considered solar cells, for the Summer and Winter solstices situations.

	Photocurrentintensity (mA/cm^2)		
	Perovskitecell	Monocrystalline Si cell	Policrystalline Si cell
Summer	26.17	32.24	23.45
Winter	13.62	17.72	12.75

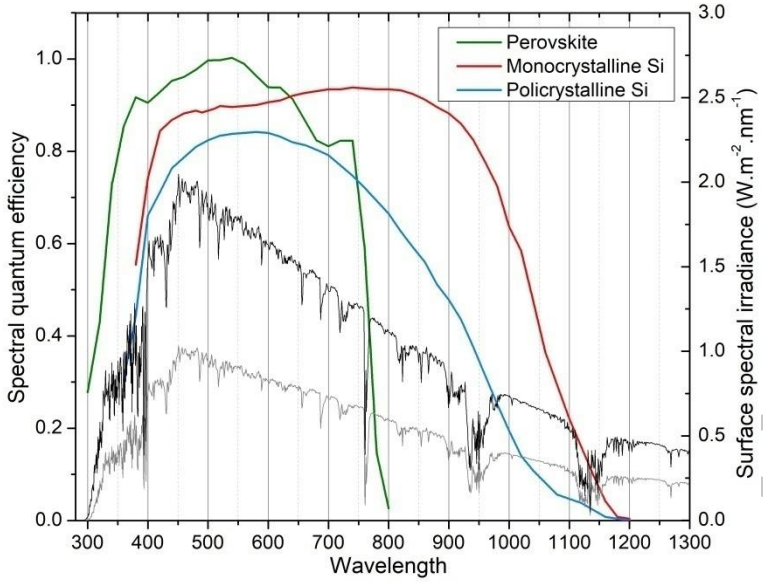

Figure 12:Spectral quantum efficiencies for 3 types of solar cells: monocrystalline Si and policrystalline Si (Salumet al., 2015), and a Ch3NH3PbI3 perovskite cell (Zhou et al, 2014). The black line is the global horizontal surface spectral irradiance [W.m^{-2}.nm^{-1}] for Summer solstice 2015 at solar noon (21st December, 13.00 local time). The grey line corresponds to the global surface spectral irradiance for Winter solstice 2015 at solar noon (21st June 13:00 local time).

From Figure 2, the estimated useable area of the LEO 2 site is: *A = 336 Km^2= 33600 hectares*. It is possible to generate about a 1MW$_{peak}$ over an area of *1.5 hectares* (Della Ceca et al, 2018). *Also it is assumed* that *10%* of the whole terrain surface is used for other applications: routes, buildings for inverters, transmission lines,etc(actually there is more place around the borders). Taking these factors into account,a solar PV plant installed on LEO 2 available area will have a solar photoproduction power given by:

$$P_{PV} = 0.9 * \frac{A}{\frac{1.5\,Ha}{MW_{peak}}} = 20160\ MW_{peak} \qquad (2)$$

On the otherside, we employed the PVout solar map developed by the World Bank Group (https://globalsolaratlas.info), to obtain a value for the *Solar PV merit factor*. This factor characterizes the efficiency of a given solar PV site for electricity production. For LEO 2 (31.5S, 69.5°W) the calculated value is:$f_{PV,}$= 2159*KWh/KW$_{peak\ per\ year}$*.So, the electricity that can be produced annually in this site region would be:

$$E_{FV} = f_{PV} * 20160\ MW_{peak} = 43.5 \times 10^6\ MWh\ per\ year \qquad (3)$$

In table 5we comparethe Global, Direct and Diffuse irradiation and the PV merit factor values for LEO 2, with those calculated for Ouarzazate and Dubai introduced in Section 3.4.

Table 5: Comparison of the PV merit factor and Global – Direct – Diffuse solar irradiation for the site in LEO 2, with the corresponding values for Ouarzazate (Morocco) and Dubai sites, where two important Solar photovoltaic solar plants are placed. Also Global irradiation data on a surface tilted to the optimum angle for each site is included. These values are obtained using the World Bank Group calculator. (https://globalsolaratlas.info).

Site	Country	Latitude/ Longitude (°)	Altitude (m asl)	PV merit factor (KWh/KWp*per year*)	Optimum angle (º)	Solar irradiation (KWh.m^{-2} per year) Horizontal Global-Direct-Diffuse (*Global,tilted to optimum angle*)
Ouarzazate	(Morocco)	30.93°/ -6.93°	1134	1939	31	2160 – 2475 – 628 (2459)
Dubai	(U.A.E.)	25.20°/ 55.27°	10	1734	24	2117 – 1798 – 897 (2285)
LEO 2	Argentina	-31.5° -69.4°	1600	2166	30	2334 – 3127 – 394 (2689)

At present, the energetic matrix of Argentina is mainly based on the generation of electricity by burning fossil fuel (althoughthere are other types of electricity sources, hydroelectric, nuclear, etc).Therefore, the introduction of large scale solar power plants in the LEO 2 region would be a very important factor in the transformation of this matrix towards cleaner and renewable energy sources.

Considering the conversion coefficient between a unit of mixed electric energy (renewable and non renewable) of the country and a unit of emited greenhouse gases (GHG), $f_{E,GHG}(Arg) = 0.5328$ *tons of* CO_{2eq}*/MWh,* the solar PV clean electricity production in LEO 2, will avoid the annual emission of the following mass of GHG:

$$M(GHG)_{FV} = f_{E,GHG}(Arg) * E_{FV} = 23.2 * 10^6 \text{ tons } CO_{2eq} \text{ per year.} \qquad (4)$$

This result considers the reduction of main GHG if the total area of LEO 2 will be used to generate PV energy, with the parameters considered before. The value is expressed in units of "*tons of CO_{2eq} per year*", where the sub-index "*eq*" indicates that other GHG are considered through their Global Warming Potential (within a 100 year horizon), including mainly Methane (CH_4) and Nitrous oxide (N_2O)(IPCC, 2015).

4. Conclusions

The following conclusions can be derived from this study, in relation to the promising characteristics of LEO 2 atmosphere, for the placement of *astrophysical* facilities:

a. Mean atmospheric UV and visible total transmittance is high, 76.08% in Summer time (December) and 67.10% in Winter time (June). Rayleigh scattering is the most important contribution to the photon attenuation, aerosol increases its absorption as the solar radiation wavelengths decrease, uniformly mixed gases and water vapor contributions are important in the visible range, only in certain wavelength absorption bands and Ozone significantly absorbs UV radiation below 330 nm.

b. The meteorological variables (determined with ground as well as satellite instruments): ambient temperature, relative humidity, wind speed, precipitable water and aerosol contents and cloud coverage fraction are very appropriate for an astrophysical observatory placement.

c. We like to point out that the high quality of the air at LEO 2 site is also of importance as a reference for the study of clear sky conditions at present and the preservation of pristine skies (without antropogenic pollution) for future generations.

d. Besides adequate atmospheric properties, a positive factor for the LEO 2 site, is its placement near the CASLEO Observatory, -the largest in the country (50 Km in the NNE direction from the Observatory). This is a significant advantage, mainly because there is already a scientific community (including Auger collaboration's Argentinean members) trained in Astronomy and Astrophysics,

which constitutes apositive local workforce available to carry out these type of projects.

With respect to *solar power plants* facilities:

e. A large and rather flat surface is available at the LEO 2 site, in the Andes region, where high mountains exist (with peaks as high as 6000 m or even more).

f. Very good mean annual solar global horizontal and tilted to optimum angle irradiations are present at the LEO 2 site, in comparison with other African (Ouarzazate, Morocco) and Asian (Dubai) sites. The total horizontal and tilted to the optimum angle) solar irradiations and PV merit factor, are higher in 8.1 %, 9.4% and 11.7%, respectively, with respect to the African site and are higher in 10.3%, 17.7% and 24.9%, respectively, with respect to the Asian site. A model calculation test was done in order to determine the possible photocurrent to be obtained at LEO 2 site, considering different solar cells (monocrystalline Si, polycrystalline Si and perovskite).

In conclusion, the LEO 2 proposed site in the Argentina East Andes range is well suited for the placement of Astrophysical facilities, as well as Photovoltaic solar power plants. In the last case, this clean and renewable energy source could increase significantly its contribution to the Argentina electrical energy matrix mix (mainly based on fossil fuels) and to decrease the GHG emissions, to mitigate climate change.

Acknowledgements

We like to thanks to the following institutions for their support to the present work: CONICET (Research Project PIP 0405) and Universidad Nacional de Rosario. Part of this work (the measurement of meteorological variables and night cloud coverage) was performed in the framework of the "*Characterization of sites for CTA International Collaboration*" project. We also like to thanks to two anonymous reviewers for their contribution to the improvement of the present manuscript.

References

Allekote I., De La Vega G., Etchegoyen A., García B., Mancilla A., Maya J., Ravignani D., Rovero A. forthe CTA consortium. (2013) "*Sites in Argentina for the Cherenkov Telescope Array Project*".Proceedings of 33rd International cosmic ray Conference ICRC, Rio de Janeiro. https://arxiv.org/pdf/1307.5014.pdf (visited 27/3/2018).

Cede A, Luccini E, Piacentini R D, Nuñez L y Blumthaler M. (2002) "Effects of clouds on erythemal and total irradiance as derived from data of the Argentine Network".*Geophysical Research Letters* 24,2002GR015708.

Cede A, Luccini E, Nuñez L ,Piacentini R D y Blumthaler M, (2002b) "Monitoring of Erythemal Irradiance in the Argentina Ultraviolet Network". Journal of Geophysical Research, 107, D13 (DOI: 2002/2001JD001206).

Della Ceca L.S, Micheletti M.I, Freire M., Garcia B., Mancilla A., Salum G.M., Crinó E, and Piacentini R.D. (2018) "Solar and climatic high performance factors for the placement of solar power plants in Argentina Andes sites. Comparison with African and Asian sites". J of Solar Engineering, published online 7th December 2018. DOI: 10.1115/1.4042203.

Draxler, R.R. and Rolph, G.D. (2004) "Description of the HYSPLIT_4 modeling system", NOAA Technical memorandum ERL ARL-224.

Gueymard C.A., (1995) "SMARTS, a simple model of the atmospheric radiative transfer of sunshine, algorithms and performance assessment", Technical Report No FSEC-PF 270-95. Cocoa FL: Florida Solar Energy Center.

Heim, M., Mullinsb, B.J., Umhauera, H., Kasper, G., (2008).” Performance evaluation of three optical particle counters with an efficient multimodal calibration method”.Aerosol Science. 39, 1019–1031.

Intergovernmental Panel on Climate Change(IPCC), Working Group I. (2013) “Climate change 2013: The physical science basis”. Cambridge University Press, page 714, 2013 (https://www.ipcc.ch/site/assets/uploads/2018/02/WG1AR5_all_final.pdf).

Ipiña, A., Salum, G.M., Crinó, E. and Piacentini, R.D. (2012). “Satellite and ground detection of very dense smoke clouds produced on the islands of the Paraná river delta that affected a large region in Central Argentina”. *Advances in Space Research*, 49 (5) 966-977.(DOI:10.1016/j.asr.2011.12.009).

Maier G., Arrabito L., Bernlohr, K., Bregeon, J., Di Pierro, J., Hassan, T., Jogler, T., Hinton, J., Moralejo, A., Wood, M. for the CTA consortium. (2015) ”*Montecarlo performance studies of candidates sites for the Cherenkov Telescope Array*”. Proceedings of 34th Cosmic Ray Conference. 30th July – 6th August 2015, The Hague, The Netherlands. https://arxiv.org/pdf/1508.06042.pdf (visited 27/3/2018).

Mandat D., Miroslav P., Miroslav H., SchovanekMiroslav P., Prouza M., Travnicek P., Janecek P., Ebr J., Doro J., Gaug M., forthe CTA consortium. (2015) “All-Sky Camera forthe CTA atmospheric calibration work package”. In: EPJ Web of conference 89 03007. Published online 26 March 2015, DOI: 10.1051/epjconf/20158903007

Micheletti M.I., Loudec K., Freire M. M., Vitale P., Piacentini R.D. (2017)“Aerosol concentration measurements and correlations with air mass trajectories at the Pierre Auger Observatory”. European Physical Journal Plus. 2017.

Otero, L., Ristori, P., D'Elía R., Pallotta, J., Quel, P. for the CTA consortium. (2013) "*Study of CASLEO, clear sky aerosol loads in 2011 for one year of AERONET quality assured data*". Proceedings of 33rd International cosmic ray Conference ICRC, Rio de Janeiro.https://arxiv.org/pdf/1307.5129.pdf (visited 27/3/2018).

Piacentini, R.D., Cede, A., Bárcena, H. (2003) "Extreme solar global and UV irradiances due to cloud effect measured near the summer solstice at the high altitude desertic plateau Puna of Atacama". Journal of Atmospheric and Solar TerrestrialPhysics, 65, 727-731.

Piacentini R D, Crino E, Sirur Flores J y Ginzburg M. (2002) "Intercomparison between TOMS/NASA and ground based ozone measurements in the Southern Hemisphere". *Advances in Space Research*, 29, 1343-1348.

Piacentini, R.D, García, B, Micheletti, M.I, Salum, G, Freire, M, Maya, J, Mancilla, A, Crino, E, Mandat, D, Pech and M, Bulik, T. (2016) «Selection of astrophysical/astronomical/solar sites at the Argentina East Andes range taking into account atmospheric components». *Advances in Space Research*, 57, (12) 2559-2574.

Piacentini R D, M. Freire, M.I. Micheletti, G.M. Salum, A. Mancilla and B. García, FOR THE CTA CONSORTIUM, (2013) "Typicalatmospheric aerosol behaviour at the Cherenkov Telescope Array candidate sites in Argentina". Proceedings 33rd ICRC (International Cosmic Ray Conference), Rio de Janeiro, July 2013.

Piacentini, R D, Luccini E, Albizatti E, Alfano O y Herman J.(2002b) "Solar ultraviolet radiation incident in clearsky days on Rosario, Argentina". J. Geophysical Research, D15, 2001JD000586.

Salum G. M., Vilela O, Pedrosa M., Cruceño J. and Piacentini R. (2015) “Spectral solar irradiance, atmospheric componenet and its relation with the production of photovoltaic current”. *Proceedings of the Solar World Conference* 2015, 8-12 november 2015, Daegu, Korea.

Vincent S., for the CTA Consortium (2013) “Atmospheric considerations for the CTA site search”, Proceeding of the ATMOHEAD Workshop, Saclay (Paris), 10-12 june 2013.

Zhou H., Chen Q., Li G., Luo S., Song T.B., Duan H.S, Hong Z., You J, Liu Y., Yang Y. (2014) “*Interface engineering of highly efficient perovskite solar cells*” Science 345 (6196) 542-546. DOI: 10.1126/science.1254050.

Highlights:

- Atmospheric components studied on an Argentinean Andean site
- Site analysis for the placement of PV power plants and astrophysical observatories..
- Comparision with african and asian sites.
- The studied site “Leoncito 2” presents very good conditions for the placement of the mentioned facilities.